Magnetic-field-induced control of breather dynamics in a single plaquette of Josephson junctions

M. V. Fistul, S. Flach, and A. Benabdallah
Max-Planck-Institut für Physik komplexer Systeme, Nöthnitzer Straße 38, D-01187 Dresden, Germany
(Received 18 September 2001; revised manuscript received 2 November 2001; published 8 April 2002)

We present a theoretical study of *inhomogeneous* dynamic (resistive) states in a single plaquette consisting of three Josephson junctions. Resonant interactions of such a breather state with electromagnetic oscillations manifest themselves by resonant current steps and voltage jumps in the current-voltage characteristics. An externally applied magnetic field leads to a variation of the relative shift between the Josephson current oscillations of two resistive junctions. By making use of the rotation wave approximation analysis and direct numerical simulations we show that this effect allows to effectively control the breather instabilities, e.g., to increase (decrease) the height of the resonant steps and to suppress the voltage jumps in the current-voltage characteristics.

DOI: 10.1103/PhysRevE.65.046616 PACS number(s): 74.50.+r, 05.45.−a

Discrete Josephson coupled systems have recently attracted a lot of attention due to the prediction [1–3] and the following observation of *intrinsic dynamic localized* states [4–7]. These breather states appear in homogeneously dc current driven Josephson junction ladders and arrays in the form of various *spatially inhomogeneous* voltage patterns. These voltage patterns are characterized by a few junctions being in the resistive (whirling) state while the rest of all junctions reside in the superconducting (libration) states. The breather states manifest themselves through additional branches in the current-voltage (I-V) characteristics of a system [4–7] and, moreover, can be directly visualized by using the low temperature scanning microscopy technique [4,5]. More complex intrinsic dynamic localized states also appear in the process of row switching in two-dimensional Josephson junction arrays as a meandering of resistive paths [8]. Note here, that the origin of such a dynamic localization is not the presence of disorder but a peculiar interplay between nonlinearity and discreteness [9], and therefore, breather states can play the same important role for Josephson junction arrays (and in particular, for Josephson junction ladders) as Josephson vortices do for long Josephson junctions and parallel arrays [10].

The dynamics of breather states crucially depend on how these states interact with other dynamical modes of the system, e.g., electromagnetic waves or localized electromagnetic oscillations. If such an interaction is weak, the amplitudes of ac currents are small, the breather state has a simple dynamical structure, and the current-voltage (I-V) curve displays a linear branch. However, by variation of an externally applied dc bias current a breather state may be tuned into resonance with linear electromagnetic excitations. It was predicted in Ref. [7] and carefully studied in Refs. [11,12] that the resonant interaction of the breather state with electromagnetic excitations leads to resonant steps (a sharp current increase) and various switching phenomena between different resistive states (voltage jumps) in the I-V curves.

The simplest case where inhomogeneous resistive states can be obtained [3,12], is a dc current driven single anisotropic plaquette containing three Josephson junctions, as presented in Fig. 1. It consists of two *vertical* junctions parallel to the bias current γ direction, and a *horizontal* junction in the transverse direction. The dynamics of the system is determined by two parameters: the anisotropy $\eta = I_{cH}/I_{cV}$, where I_{cH} and I_{cV} are, respectively, the critical currents of horizontal and vertical junctions, and the discreteness parameter (normalized inductance of the cell), β_L.

In Ref. [12] we have shown that inhomogeneous resistive states can be observed in this system as the anisotropy η is not large. These two breather states are characterized by only one (left or right) vertical junction and the horizontal junction being resistive. We also found various further features of the states, e.g., resonant current steps and voltage jumps to the superconducting state or to the homogeneous whirling state, in the I-V curves. These features can be considered ''fingerprints'' of the resonant interaction of the breather state with electromagnetic oscillations (EO's). The necessary condition of the appearance of resonant interaction is the matching of the breather frequency Ω or its higher harmonics with the frequencies of EO's, $\omega_{\pm}$ [12]. The different types of resonances are classified as *primary* resonances ($\omega_{\pm} = m\Omega$), *parametric* resonances [$\omega_{\pm} = (m + \frac{1}{2})\Omega$] and *combination* resonances ($m\Omega = \omega_{+} \pm \omega_{-}$). Note here that the dc voltage drop is determined by the breather frequency as $V = \hbar\Omega/2e$. The frequencies of EO's, and therefore the voltage positions of the resonances, depend strongly on the parameters η and β_L. The presence (or absence) of resonant features in the I-V curves is affected also by the *strength* of the resonant interaction, i.e., a possibility to excite the EO's by the

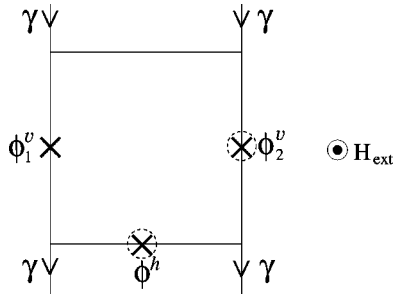

FIG. 1. Sketch of the plaquette with three Josephson junctions (marked by crosses) in the presence of uniform dc bias γ and an externally applied magnetic field H_{ext}. Dashed circles denote junctions in the resistive (whirling) state.

breather state. However, a theoretical analysis of the strength of the resonant interaction has not been carried out, and moreover, the dependence of resonant features on an externally applied magnetic field has not been investigated.

In this paper, we report on the properties of breather states or even more specifically, on the resonant interaction of the breather states with EO's in the presence of an externally applied magnetic field. We show that the applied magnetic field allows to control the strength of the resonant interaction, and correspondingly the appearance (disappearance) of voltage jumps and resonant steps in the *I-V* curves, just by a fine tuning of the relative phase shift between the Josephson current oscillations of the two resistive junctions.

In order to quantitatively characterize the magnetic field induced control we write the set of equations for the time-dependent Josephson phases ϕ_1^v, ϕ_2^v, and ϕ^h:

$$\begin{aligned}
\mathcal{N}(\phi_1^v) &= \gamma - \frac{1}{\beta_L}(\phi_1^v - \phi_2^v + \phi^h + 2\pi f),\\
\mathcal{N}(\phi_2^v) &= \gamma + \frac{1}{\beta_L}(\phi_1^v - \phi_2^v + \phi^h + 2\pi f),\\
\mathcal{N}(\phi^h) &= -\frac{1}{\eta\beta_L}(\phi_1^v - \phi_2^v + \phi^h + 2\pi f),
\end{aligned} \tag{1}$$

where the nonlinear operator $\mathcal{N}(\phi) = \ddot{\phi} + \alpha\dot{\phi} + \sin(\phi)$, and the dissipation parameter α determines the effective damping in the system. Here, we use the inverse of the plasma frequency ω_p as the unit of time. The externally applied magnetic field $H_{\rm ext}$ is characterized by the frustration $f = \Phi_{\rm ext}/\Phi_0$, i.e., the magnetic flux threading the cell normalized to the magnetic flux quantum. These dynamic equations have been derived in Ref. [12], using the resistively shunted model for Josephson junctions, the Kirchhoff's current laws, and the flux quantization law.

The Josephson phases are naturally decomposed as follows (below we consider a particular breather case as the left vertical junction is in the superconducting state):

$$\begin{aligned}
\phi_1^v(t) &\approx c_1 + \delta_1^v(t),\\
\phi_2^v(t) &\approx \Omega t + c_2 + \delta_2^v(t),\\
\phi^h(t) &\approx \Omega t + \delta^h(t),
\end{aligned} \tag{2}$$

where the dc bias dependent breather frequency Ω and the phase shifts c_1 and c_2 are obtained using a *dc analysis* [12], i.e., neglecting the Josephson phase oscillations $\delta(t)$:

$$\begin{aligned}
\Omega &= \frac{\gamma}{\alpha(1+\eta)},\\
c_1 &= \arcsin\left(\frac{1+2\eta}{1+\eta}\gamma\right),\\
c_2 &= c_1 + \frac{\beta_L\gamma\eta}{1+\eta} + 2\pi f.
\end{aligned} \tag{3}$$

In Eq. (2), $\delta_{1,2}^v(t)$, $\delta^h(t)$ correspond to EO's excited in the presence of the breather state. By making use of the linearization of Eq. (1) around the breather state (2) we obtain

$$\begin{aligned}
\ddot{\delta}_1^v + \alpha\dot{\delta}_1^v + \cos(c_1)\,\delta_1^v &= -\frac{1}{\beta_L}(\delta_1^v - \delta_2^v + \delta^h),\\
\ddot{\delta}_2^v + \alpha\dot{\delta}_2^v + \cos(\Omega t + c_2)\,\delta_2^v &\\
= -\sin(\Omega t + c_2) + \frac{1}{\beta_L}(\delta_1^v - \delta_2^v + \delta^h),&\\
\ddot{\delta}^h + \alpha\dot{\delta}^h + \cos(\Omega t)\,\delta^h &= -\sin(\Omega t) - \frac{1}{\eta\beta_L}(\delta_1^v - \delta_2^v + \delta^h).
\end{aligned} \tag{4}$$

Two characteristic frequencies of EO's are derived by neglecting the damping ($\alpha \ll 1$) and time-dependent terms in Eq. (4) as

$$\begin{aligned}
|\omega_\pm| &= \sqrt{F \pm \sqrt{F^2 - G}},\\
F &= \frac{1}{2}\cos(c_1) + \frac{1+2\eta}{2\eta\beta_L},\\
G &= \cos(c_1)\frac{(1+\eta)}{\eta\beta_L}.
\end{aligned} \tag{5}$$

Thus, as the resonant condition is valid, $\Omega = \omega_\pm$, a primary resonance appears and the *I-V* curve displays a resonant current step. The magnitude of the resonant step is found as

$$\Delta\gamma = \langle \delta_2^v(t)\cos(\Omega t + c_2)\rangle, \tag{6}$$

where $\langle \ldots \rangle$ means the time-average procedure. At the resonance the EO's have a form $\delta_{1,2}^v, \delta^h \simeq e^{i\Omega t}$. Using the rotation wave approximation method elaborated in Ref. [13], i.e., neglecting all nonresonant terms, we find that the amplitudes of EO's and correspondingly, the strength of the primary resonance are determined by the *difference* of two Josephson current oscillations: $\sin(\Omega t + c_2) - \sin(\Omega t)$ [see the right-hand side of Eq. (4)]. It leads to the magnetic field dependent magnitude of the resonant step $\Delta\gamma$:

$$\Delta\gamma \propto \left|\sin\frac{c_2}{2}\right| = \left|\sin\left(\frac{c_1}{2} + \frac{\beta_L\gamma\eta}{2(1+\eta)} + \pi f\right)\right|. \tag{7}$$

The dependence of $\Delta\gamma$ on f is not symmetric with respect to the value of $f = 0$, which is due to the intrinsic inhomogeneity of the breather state, i.e., the phase shift c_2 is not zero even in the absence of an externally applied magnetic field.

Next, we turn to the parametric resonant interaction of the breather state with EO's, as $\Omega = 2\omega_\pm$. In order to analyze this case we introduce the new variables $D(t) = \delta_2^v(t) - \delta^h(t)$ and $S(t) = \delta_2^v(t) + \delta^h(t)$. The equations for $D(t)$ and $S(t)$ are given by

$$\ddot{D} + \alpha\dot{D} + \omega_\pm^2 D = -Dh_1(t) + Sh_2(t),$$

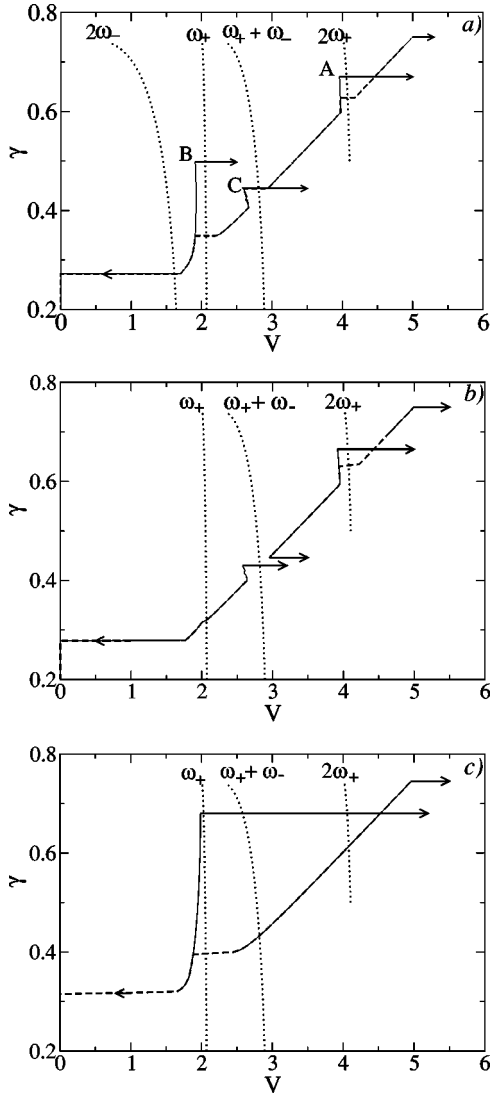

FIG. 2. *I-V* characteristics of a breather state for $\beta_L=1$, $\alpha=0.1$, and $\eta=0.5$. The values of the magnetic field are (a) $f=0$, (b) $f=-0.1$, and (c) $f=0.4$. The thin solid (dashed) lines show the dc bias increase (decrease). The dotted lines show the dependence of the characteristic frequency combinations of EO's on the dc bias γ [Eq. (5)]. Arrows indicate the various switching processes: to the homogeneous whirling state or to the superconducting state.

$$\ddot{S}+\alpha\dot{S}+\frac{\eta-1}{\eta+1}\omega_{\pm}^{2}D=-Sh_1(t)+Dh_2(t), \tag{8}$$

where the time-dependent coefficients $h_1(t)=\cos(c_2/2)\cos(\Omega t)$ and $h_2(t)=\sin(c_2/2)\sin(\Omega t)$. Note here that we neglected all nonresonant terms in Eq. (4) [14]. Similarly to a well known case of a parametrically driven harmonic oscillator [15] we find that in the dissipative case with two degrees of freedom [Eq. (8)] the breather state can become parametrically unstable, when the Josephson phases are

$$D(t),S(t)\simeq e^{i(\Omega t/2)+\lambda t} \tag{9}$$

with $\lambda>0$. This instability depends on the amplitudes of ac Josephson oscillations $h_1(t)$ and $h_2(t)$, and therefore, is determined by the phase shift c_2. Substituting the Josephson phases (9) to (8) we obtain the instability condition

$$h_{\rm eff}(f)=\sqrt{(1-\eta)^2+4\eta\cos^2(c_2/2)}>\alpha\Omega. \tag{10}$$

The left-hand side of this equation determines the effective amplitude of the parametric Josephson current oscillations $h_{eff}(f)$ in the same manner as the effective amplitude $\sin(c_2/2)$ of primary Josephson current oscillations [see Eq. (7)].

The strength of the combination resonance as $\Omega=\omega_+\pm\omega_-$, is also determined by the parameter $h_{\rm eff}(f)$. By taking the Josephson phases D and S in the form $D(t)\simeq e^{i\omega_+ t+\lambda t}$ and $S(t)\simeq e^{i\omega_- t+\lambda t}$, the instability condition of the combination resonance is found as

$$h_{\rm eff}(f)>\alpha\sqrt{\omega_+\omega_-}. \tag{11}$$

Thus, the applied magnetic field allows us to control the strength of the parametric and combination resonances through the magnetic field dependent phase shift between two Josephson current oscillations, c_2.

To test the obtained analysis and to show how the applied magnetic field changes the *I-V* curve, we perform direct numerical simulations of Eq. (1). Details of the numerical procedure were given elsewhere [12]. To establish a large dc

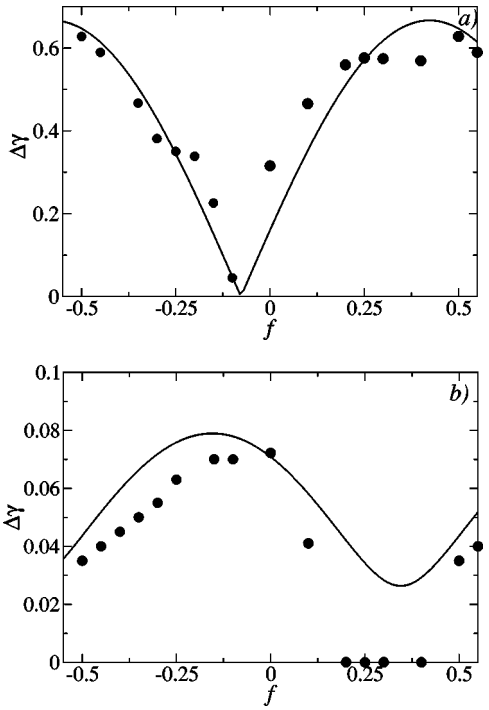

FIG. 3. The dependence of the magnitude of the resonant steps on the frustration *f*: (a) the lower resonant step (primary resonance, *B*). The numerical results (circles) and the analytical prediction [Eq. (7)] are shown correspondingly by circles and solid lines. (b) The upper resonant step (parametric resonance, *A*), the numerical results (circles), and the analytical prediction (solid line) based on the expression for $h_{\rm eff}(f)$ [Eq. (10)] are shown.

current bias region where various types of resonances occur, we use the discreteness parameter $\beta_L = 1$ and the anisotropy $\eta = 0.5$. We decreased (increased) the dc bias current and calculated the dc voltage $V = \langle \dot{\phi}_2^v \rangle$. Numerically simulated I-V curves for different values of the applied magnetic field are shown in Fig. 2.

In the absence of the magnetic field [see Fig. 2(a)] we observed two resonant steps labeled as A and B, and the switching phenomenon (the voltage jump to the homogeneous resistive state) labeled as C. All types of resonant interactions of the breather state with EO's are present in this I-V curve: the parametric resonance A leads to the the resonant step at upper values of the dc bias γ, the primary resonance B leads to the resonant step at lower values of the dc bias γ, and the voltage jump C is the consequence of the combination resonance [12].

In the presence of an applied magnetic field we find that the I-V curve changes drastically. Thus, for a small magnetic field $f = -0.1$ the lower voltage resonant step B practically disappears, but the switching phenomenon C becomes even stronger [Fig. 2(b)]. In the opposite limit of a large magnetic field, as $f = 0.4$, the parametric and the combination resonances (A, C) disappear from the I-V curve but the magnitude of the lower voltage resonant step B (primary resonance) increases [Fig. 2(c)].

The dependence of the magnitude of the lower resonant step on the frustration displays a minimum on small negative values of f and reaches a maximum as $f \simeq 0.4$ [circles in Fig. 3(a)]. Thus, in particular the dependence $\Delta\gamma(f)$ is not symmetric with respect to $f = 0$, which is in good accord with the theoretical analysis [Eq. (7) and solid line in Fig. 3(a)].

The numerically simulated dependence of the magnitude of the upper resonant step A is shown in Fig. 3(b). This dependence displays a peculiar oscillation and is in qualitative agreement with the magnetic field dependence of $h_{\mathrm{eff}}(f)$. Moreover, as suggested by the inequality in Eq. (10) in the region of frustration $0.2 < f < 0.37$ a specific ''window'' of magnetic field occurs. In this region of the magnetic field the parametric resonant interaction is very weak and the resonant step A disappears from the I-V curve. Note here that the width of the ''windows'' increases with the damping parameter α [Eq. (10)], and this allows for an accurate measurement of damping at low temperatures as α is very small.

In the same region of frustration, a similar window exists for the combination resonance and correspondingly the switching of the breather state to the homogeneous resistive state is suppressed. This effect has a peculiar consequence. Because of the instability of the breather state and the corresponding switching to the homogeneous resistive state [see Fig. 2(b)], it can be very hard to experimentally observe the lower part of the I-V curve. However, in the presence of a magnetic field the breather can pass this region of dc bias current and penetrate to the ''forbidden'' current region.

In conclusion we presented an analysis and direct numerical simulations of the inhomogeneous resistive state in a single plaquette consisting of three Josephson junctions. We find that the I-V curve of such a breather state displays peculiar features, namely resonant steps and voltage jumps. The magnitudes of all features are determined by the phase shift between two Josephson current oscillations that in turn, can be controlled by an externally applied magnetic field.

The authors thank A. Miroshnichenko, F. Pignatelli, M. Schuster, and A. V. Ustinov for useful discussions. This work was supported by the European Union under the RTN Project No. LOCNET HPRN-CT-1999-00163.

[1] L.M. Floria, J.L. Marin, P.L. Martínez, F. Falo, and S. Aubry, Europhys. Lett. **36**, 539 (1996).
[2] S. Flach and M. Spicci, J. Phys.: Condens. Matter **11**, 321 (1999).
[3] J.J. Mazo, E. Trías, and T.P. Orlando, Phys. Rev. B **59**, 13 604 (1999).
[4] P. Binder, D. Abraimov, A.V. Ustinov, S. Flach, and Y. Zolotaryuk, Phys. Rev. Lett. **84**, 745 (2000).
[5] P. Binder, D. Abraimov, and A.V. Ustinov, Phys. Rev. E **62**, 2858 (2000).
[6] E. Trías, J.J. Mazo, and T.P. Orlando, Phys. Rev. Lett. **84**, 741 (2000).
[7] E. Trías, J.J. Mazo, A. Brinkman, and T.P. Orlando, Physica D **156**, 98 (2001).
[8] D. Abraimov, P. Caputo, G. Filatrella, M.V. Fistul, G.Yu. Logvenov, and A.V. Ustinov, Phys. Rev. Lett. **83**, 5354 (1999).
[9] S. Flach and C.R. Willis, Phys. Rep. **295**, 182 (1998).
[10] A.V. Ustinov, Physica D **123**, 315 (1998).
[11] A.E. Miroshnichenko, S. Flach, M.V. Fistul, Y. Zolotaryuk, and J.B. Page, Phys. Rev. E **64**, 066601 (2001).
[12] A. Benabdallah, M.V. Fistul, and S. Flach, Physica D **159**, 202 (2001).
[13] I.O. Kulik, Zh. Tekh. Fiz. **37**, 157 (1967) [Sov. Phys. Tech. Phys. **12**, 111 (1967)].
[14] Equations (8) are not valid in the limit of large discreteness parameter, $\beta_L \geqslant \alpha^{-1}$. However, in this limit the resonant interaction of the breather state with EO's is very weak.
[15] L.D. Landau and E.M. Lifshits, *Course of Theoretical Physics; Mechanics* (Oxford Pergamon, London, 1994).